Supporting information

Methods

Community analysis

Polymerase chain reaction (PCR) was performed with a set of primers (338F/806R) targeting the V3–V4 region of the 16S rRNA gene in a 20 μL PCR-reaction system (Table S4) before sequencing. The detail of the polymerase chain reaction (PCR) amplification method was: pre-denaturation at 94℃ for 3 min, denaturation at 94℃ for 30 s, annealing at 45℃ for 30 s, extension at 60℃ for 1 min, a total of 30 cycles, and extension at 72℃ for 2 min. The amplified 16S rDNA was sequenced using the Hi-Seq platform (Illumina Inc., USA) with a paired-end 250 strategy. The raw data were analyzed using Majorbio Cloud Platform, a free online platform. The pair-end reads were merged using FLASH (version 1.2.11), then QIIME (version 1.9.1) was used to quantify the merged sequences. UPARSE was used to cluster the effective tags into operational taxonomic units (OTUs > 97% similarity). After alignment by PyNAST, the representative sequences were assigned with the Silva database for taxonomic classification.

Reactive oxygen species detection

The fluorescent probe 2',7'-dichlorodihydrofluorescein diacetate (DCFH-DA, Beyotime, China) was used to detect the total reactive oxygen produced by microorganisms. A bacterial culture grown for 24 h in the dark was centrifuged at 5000 r/min for 5 min, and the bacterial pellet was collected and resuspended in fresh medium to an Abs_{600} value of 1. Cells were then incubated with 10 μmol/L DCFH-DA in the dark at 37℃ for 30 min, and shaken manually every 5 min to load the probe into the cell. After loading the probe, it was washed with fresh medium three times to remove the excess unloaded probe to reduce background interference and resuspend it in an equal volume of fresh medium. Then the cells were exposed to light for 2 h, and cultured in the dark for 2 h as a negative control. In the manganese-added group, $MnSO_4$ was added (final concentration of 1 mmol/L) after the probe loading and then cultured in the light and dark, respectively. Specifically, the Rosup reagent was added under dark culture as a positive control. After light exposure, DCF fluorescence intensity was detected using a microplate analyzer (Spark, TECAN, Austria. Excitation and emission wavelength were 488 nm and 525 nm, respectively). The change in fluorescence intensity between the experimental group and the negative control group was calculated.

Manganese oxides characterization

After 8 days of light culture, the culture medium was centrifuged at 6000 r/min for 10 min to collect the Mn(III/IV) oxides. The precipitates were washed twice with ultrapure water, freeze-

dried, and ground to powder, in preparation for SEM observation, and XRD, XPS, and UV-visible diffuse reflectance analysis.

The morphology of biogenic Mn(III/IV) oxides was investigated by scanning electron microscope (SEM) (Hitachi S-4800, Japan). The crystallinity of biogenic Mn(III/IV) oxides was detected by powder X-ray diffractometer (XRD, Panalytical X'Pert Pro, Netherlands). The test voltage and current were 40 kV and 40 mA, respectively, using Cu Kα radiation (λ = 1.54 Å). The step length was 0.02°, the scanning speed was 4 (°)/min, and the scanning range is 5°–80°. X-ray photoelectron spectroscopy (XPS) (Shimadzu Axis Supra, Japan) analysis was carried out using nonmonochromatic Al Kα X-rays (hν = 1486.6 eV) as the excitation source (X-ray tube power of 150 W, vacuum of 1.3×10^{-7} Pa, room temperature). All peak energies obtained in this study were calibrated based on the energy of external carbon (284.8 eV). The optical absorption properties of the biogenic Mn(III/IV) oxides were determined via a UV–Vis spectrometer (Shimadzu UV-3600, Japan) with the baseline of $BaSO_4$ as a reference. The spectral data were collected within the range of 200–1000 nm, and the spectral bandwidth was set at 4.0 nm with a scan rate of 400 nm/min. The recorded spectral data interval was set at 1.0 nm.

Preparation of the Mn(III/IV) oxides electrodes

The Mn(III/IV) oxides electrodes were prepared by using the Mn(III/IV) oxides powder sample. The preparation of the powder was the same as that for the oxides characterization. Fifty milligrams of freeze-dried Mn(III/IV) oxides powder was mixed with 400 μL anhydrous ethanol and 10 μL 5% Nafion to make an oxides paste. Then, 5 μL of oxides paste was evenly smeared on the transparent conductive ITO electrode (tin oxide, purchased from Zhuhai Kaivo Optoelectronic Technology Company, China, electrode effective area 0.5×0.5 cm^2). Before use, the ITO was sonicated in 1% hydrochloric acid for 5 minutes and then ultrasonically cleaning with acetone, ethanol, and ultrapure water for 30 minutes gradually, finally, dried with nitrogen. The Mn(III/IV) oxides electrodes were dried in air for 30 min before electrochemical measurements.

Photoelectrochemical characterization

The photocurrent-time curve is used to characterize the photoelectric response of Mn(III/IV) oxides samples, which provides information on the photoelectric response performance and photostability of semiconductor electrodes. The photochemical tests were carried out in a standard three-electrode system, which consisted of a Mn(III/IV) oxides electrode as the working electrode, an Ag/AgCl electrode as the reference electrode, and a platinum wire as the counter electrode. A 0.1 mol/L Na_2SO_4 aqueous solution with a pH of 7 was used as the electrolyte. A Xenon lamp (Perfect Light Company Ltd., China) was used as the excitation source (an optical filter was used to cut off wavelength under 400 nm). The light was irradiated on the Mn(III/IV) oxides electrode from the front face, and the intensity of the incident light was adjusted to 50 mW/cm^2. The photocurrent-time response of the Mn(III/IV) oxides electrode was measured by chronoamperometry with a CHI 660D electrochemical workstation (Shanghai Chenhua Apparatus Corporation, China) at a constant potential of 1 V (vs. Ag/AgCl), and the hand-controlled shutter was used to obtain the light and dark response curves.

The Mott-Schottky curve can determine the semiconductor type and the flat band potential. Mott–Schottky plots were measured at a frequency of 1 kHz in the same system as photocurrent-time measurements with a scan range of –0.2–0.8 V (vs. Ag/AgCl).

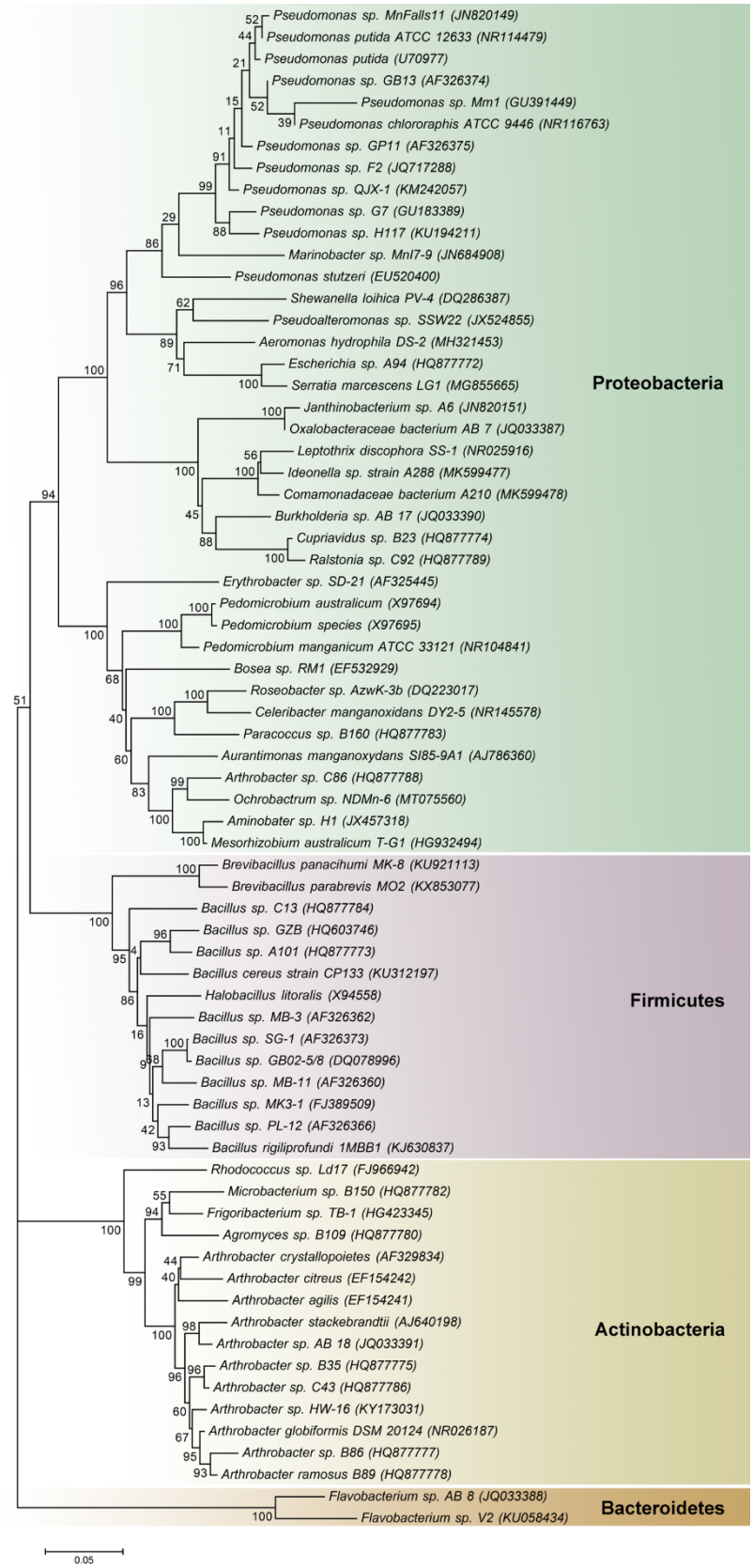

Fig. S1 Phylogenetic tree of manganese-oxidizing bacteria. Neighbor-joining tree constructed based on 16S rRNA gene, the data comes from (De Vrind et al., 1986; Adams and Ghiorse, 1987; Larsen et al., 1999; Learman et al., 2011; Liu et al., 2018; Zhang et al., 2019; Zhou and Fu, 2020).

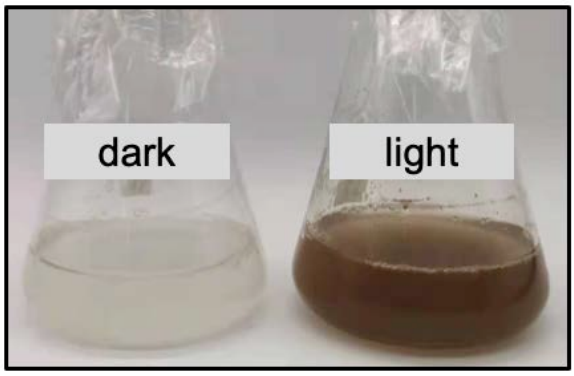

Fig. S2 The photo of culture medium after 8 days incubation under light/dark.

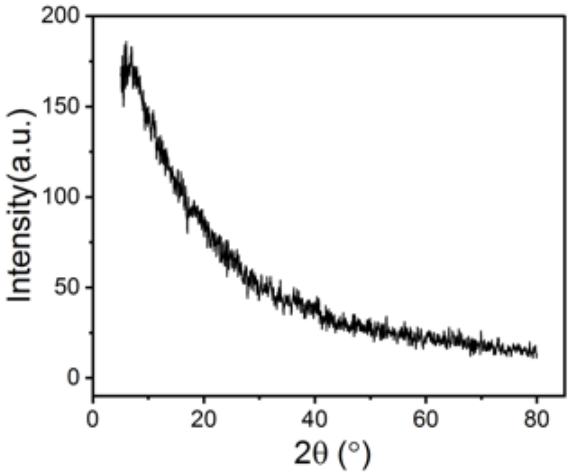

Fig. S3 XRD spectrum of biogenic Mn(III/IV) oxides under visible light.

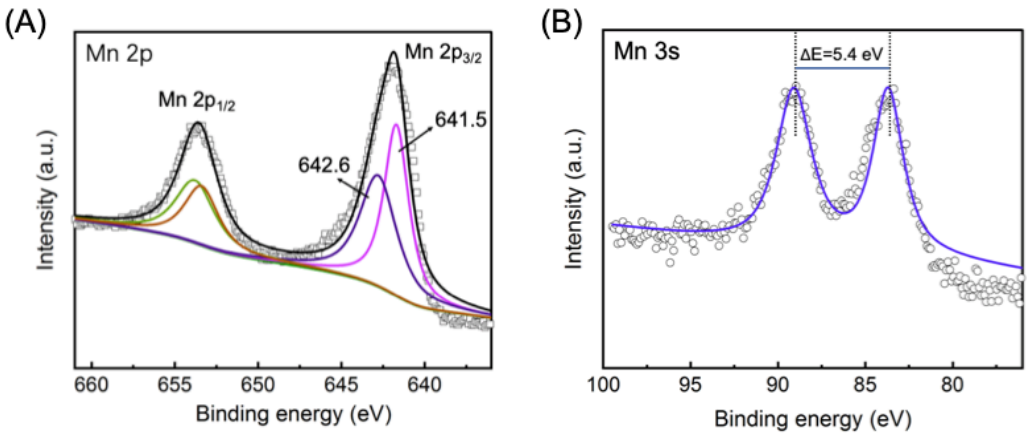

Fig. S4 XPS spectrum of biogenic Mn(III/IV) oxides under visible light. (A) Mn 2p; (B) Mn 3s.

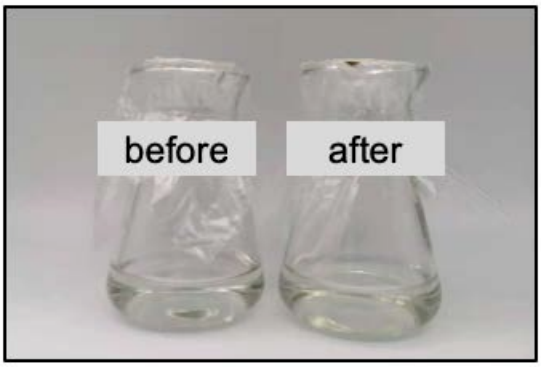

Fig. S5 The photo of cell-free filtrate containing 1 mmol/L Mn(II) ions before and after 5 days of light incubation.

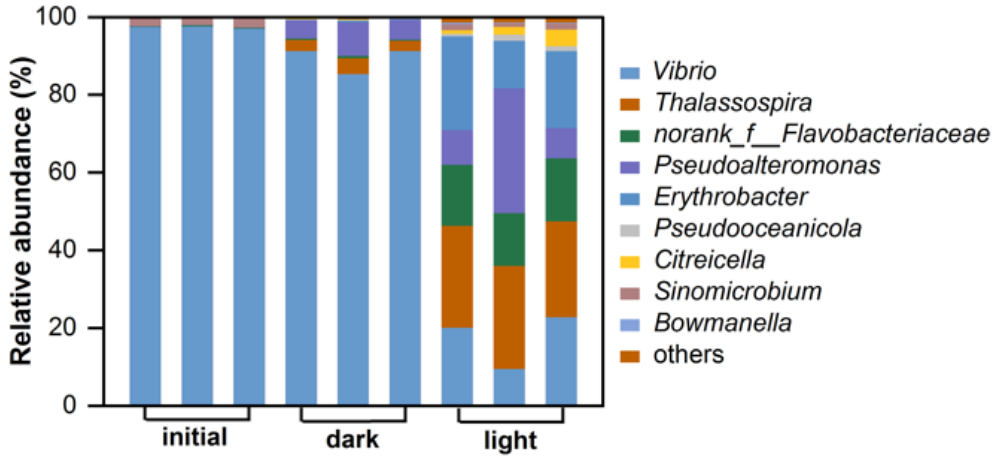

Fig. S6 Communities composition before and after light/dark culture without manganese (genus level). Cultured without Mn(II) ions in dark/light are marked dark, light, respectively. The initial inoculum is marked as initial.

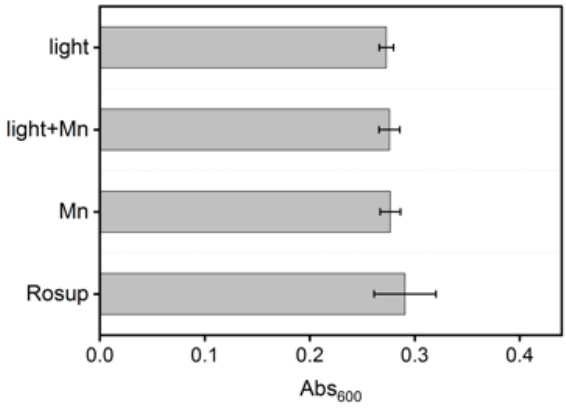

Fig. S7 Biomass of different groups for ROS test.

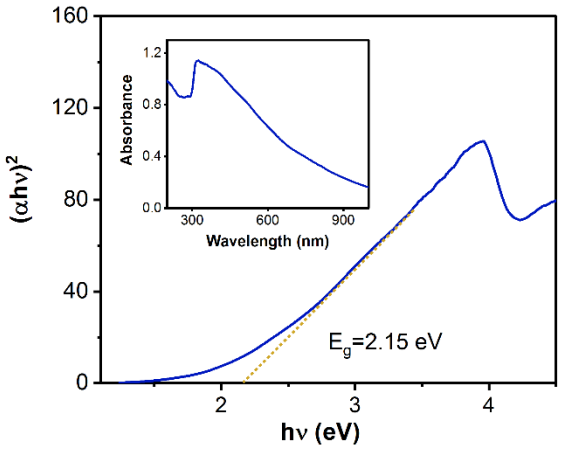

Fig. S8 Tauc plot and the UV–vis absorption spectrum (insert) of biogenic Mn(III/IV) oxides.

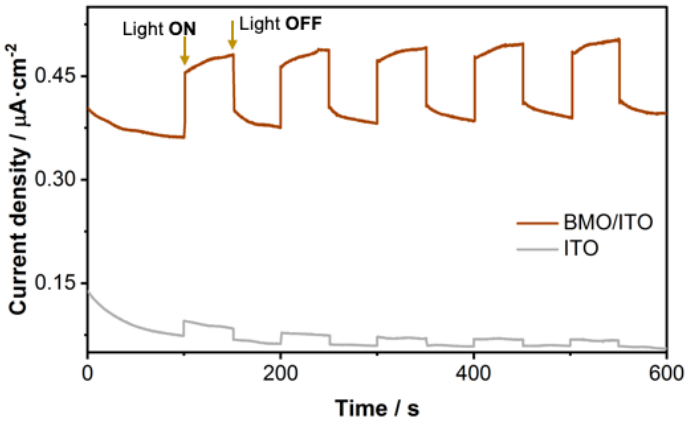

Fig. S9 Photocurrent–time behaviors of biogenic Mn(III/IV) oxides electrodes (BMO/ITO) in supporting electrolyte of 0.1 mol/L Na_2SO_4 at 0.6 V (vs. Ag/AgCl).

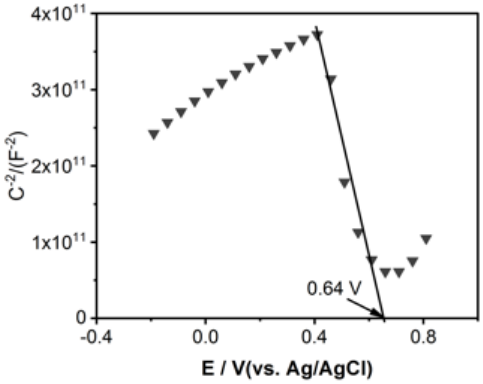

Fig. S10 Electrochemical Mott-Schottky plots of biogenic Mn(III/IV) oxides.

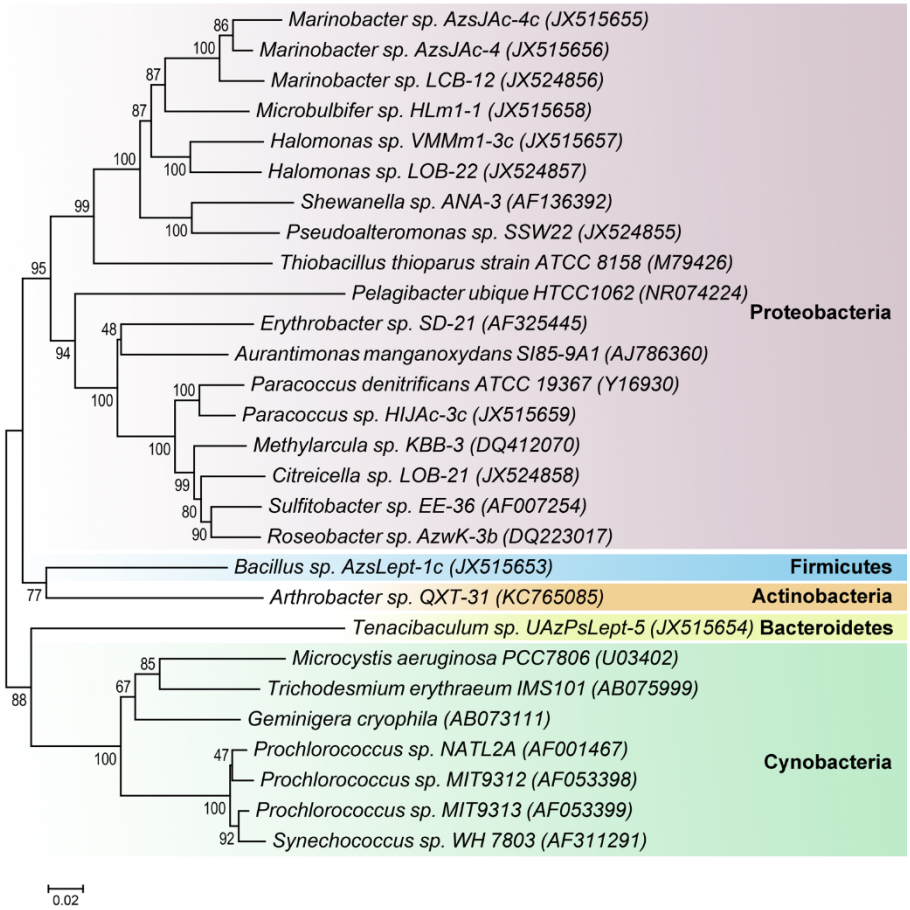

Fig. S11 Phylogenetic tree of superoxide-producing bacteria. Neighbor-joining tree constructed based on 16S rRNA gene, the data comes from (Fujii et al., 2010; Diaz et al., 2013; Roe and Barbeau, 2014; Sutherland et al., 2019; Ning et al., 2022).

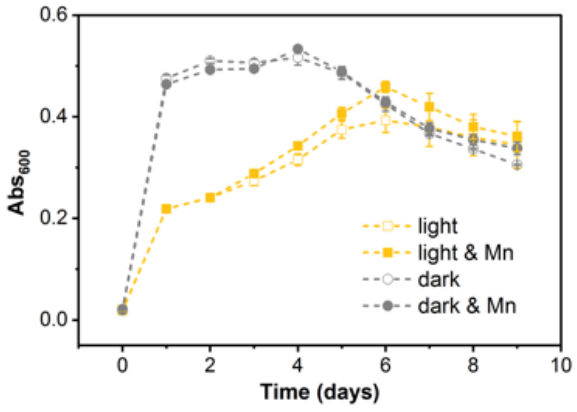

Fig. S12 Changes of biomass under different culture conditions. The absorbance of the medium at 600 nm is used to indicate the biomass. Yellow and gray represent culture under light and dark respectively; Solid and hollow symbols represent with and without Mn(II) ions, respectively. The error bar represents the standard deviation of three biological replicates.

Table S1 Composition of K-acetate medium.

Chemicals	Content (g/L)
NaCl	13.14
$MgSO_4 \cdot 7H_2O$	7.24
KCl	0.56
$CaCl_2$	0.83
NH_4Cl	0.08
Sodium acetate	0.82
Yeast extract	0.10
Hepes*	2.38

Notes: Adjust pH to 7.5 before autoclaving. All the reagents used were purchased from Sinopharm Chemical Reagent Co. LTD, China, with AR purity. * Hepes: 4-(2-hydroxyethyl)-1-piperazineethanesulfonic acid.

Table S2 Composition of artificial seawater.

Chemicals	Content (g/L)
NaCl	13.14
$MgSO_4 \cdot 7H_2O$	7.24
KCl	0.56
$CaCl_2$	0.83
NH_4Cl	0.08
Hepes*	2.38

Notes: Adjust pH to 7.5. All the reagents used were purchased from Sinopharm Chemical Reagent Co. LTD, China, with AR purity. *Hepes: 4-(2-hydroxyethyl)-1-piperazineethanesulfonic acid.

Table S3 Community richness and diversity indices for all samples.

Samples	Sequences	OTUs	Shannon	Simpson
initial 1	58684	10	0.446869	0.799737
initial 2	42377	10	0.436836	0.806151
initial 3	45018	10	0.466629	0.791814
dark 1	44654	19	0.693795	0.707644
dark 2	44761	19	0.880483	0.615306
dark 3	36446	19	0.725608	0.68649
light 1	40563	23	1.849525	0.192119
light 2	42616	22	1.783193	0.215075
light 3	53162	24	1.932588	0.176665
dark+Mn 1	43360	22	1.950253	0.210982
dark+Mn 2	42587	23	1.704472	0.319099
dark+Mn 3	43727	19	1.278305	0.487561
light+Mn 1	42731	23	1.382369	0.323103
light+Mn 2	52139	22	1.477869	0.300975
light+Mn 3	44313	24	1.565559	0.274845

Notes: Cultured with and without Mn(II) ions in dark/light are marked as dark+Mn and light+Mn, respectively. The initial inoculum is marked as initial.

Table S4 The detailed composition of reagents for the PCR amplification method.

Reagents	Value
5×FastPfu buffer	4.0 μL
2.5 mmol/L dNTPs	2.0 μL
Forward primers (5.0 μmol/L)	0.8 μL
Reverse primers (5.0 μmol/L)	0.8 μL
FastPfu Polymerase	0.4 μL
BSA	0.2 μL
Template DNA	10.0 ng

Notes: Double distilled water was added to get a final volume of 20.0 μL.

References

Adams L F, Ghiorse W C (1987). Characterization of extracellular Mn^{2+}-oxidizing activity and isolation of an Mn^{2+}-oxidizing protein from Leptothrix discophora SS-1. Journal of Bacteriology, 169(3): 1279–1285

De Vrind J P M, De Vrind-de Jong E W, De Voogt J W H, Westbroek P, Boogerd F C, Rosson R A (1986). Manganese oxidation by spores and spore coats of a marine bacillus species. Applied and Environmental Microbiology, 52(5): 1096–1100

Diaz J M, Hansel C M, Voelker B M, Mendes C M, Andeer P F, Zhang T (2013). Widespread production of extracellular superoxide by heterotrophic bacteria. Science, 340(6137): 1223–1226

Fujii M, Rose A L, Omura T, Waite T D (2010). Effect of Fe(II) and Fe(III) transformation kinetics on iron acquisition by a toxic strain of *Microcystis aeruginosa*. Environmental Science & Technology, 44(6): 1980–1986

Larsen E I, Sly L I, McEwan A G (1999). Manganese(II) adsorption and oxidation by whole cells and a membrane fraction of *Pedomicrobium* sp. ACM 3067. Archives of Microbiology, 171(4): 257–264

Learman D R, Voelker B M, Vazquez-Rodriguez A I, Hansel C M (2011). Formation of manganese oxides by bacterially generated superoxide. Nature Geoscience, 4(2): 95–98

Liu J, Wang O, Li J, Liu F (2018). Mechanisms of extracellular electron transfer in the biogeochemical manganese cycle. Acta Microbiologica Sinica, 58(4): 546–559

Ning X, Liang J, Men Y, Wang Y, Chang Y, Bai Y, Liu H, Wang A, Zhang T, Qu J (2022). Siderophores provoke extracellular superoxide production by *Arthrobacter* strains during carbon sources-level fluctuation. Environmental Microbiology, 24(2): 894–904

Roe K L, Barbeau K A (2014). Uptake mechanisms for inorganic iron and ferric citrate in *Trichodesmium erythraeum* IMS101. Metallomics, 6(11): 2042–2051

Sutherland K M, Coe A, Gast R J, Plummer S, Suffridge C P, Diaz J M, Bowman J S, Wankel S D, Hansel C M (2019). Extracellular superoxide production by key microbes in the global ocean. Limnology and Oceanography, 64(6): 2679–2693

Zhang Y, Tang Y, Qin Z, Luo P, Ma Z, Tan M, Kang H, Huang Z (2019). A novel manganese oxidizing bacterium-*Aeromonas hydrophila* strain DS02: Mn(II) oxidization and biogenic Mn oxides generation. Journal of Hazardous Materials, 367: 539–545

Zhou H, Fu C (2020). Manganese-oxidizing microbes and biogenic manganese oxides: characterization, Mn(II) oxidation mechanism and environmental relevance. Reviews in Environmental Science and Biotechnology, 19(3): 489–507